Stanford Exploration Project, Report 108, April 29, 2001, pages 1–??

A differential scheme for elastic properties of rocks with dry or saturated cracks

James G. Berryman,[1] *Steven R. Pride,*[2] *and Herbert F. Wang*[3]

ABSTRACT

Differential effective medium (DEM) theory is applied to the problem of estimating physical properties of elastic media with penny-shaped cracks, filled either with air or liquid. These cracks are assumed to be randomly oriented. It is known that such a model captures many of the essential physical features of fluid-saturated or partially saturated rocks. By making the assumption that the changes in certain factors depending only on Poisson's ratio do not strongly affect the results, it is possible to decouple the equations for bulk (K) and shear (G) modulus, and then integrate them analytically. The validity of this assumption is then tested by integrating the full DEM equations numerically. The analytical and numerical curves for both K and G are in very good agreement over the whole porosity range of interest. Justification of the Poisson's ratio approximation is also provided directly by the theory, which shows that, as porosity tends to 100%, Poisson's ratio tends towards small positive values for dry, cracked porous media and tends to one-half for liquid saturated samples. A rigorous stable fixed point is obtained for Poisson's ratio, ν_c, of dry porous media, where the location of this fixed point depends only on the shape of the voids being added. Fixed points occur at $\nu_c = 1/5$ for spheres, and $\nu_c \simeq \pi\alpha/18$ for cracks, α being the aspect ratio of penny-shaped cracks. Results for the elastic constants are then compared and contrasted with results predicted by Gassmann's equations and with results of Mavko and Jizba, for both granite-like and sandstone-like examples. Gassmann's equations do not predict the observed liquid dependence of the shear modulus G at all. Mavko and Jizba predict the observed dependence of shear modulus on liquid bulk modulus for small crack porosity, but fail to predict the observed behavior at higher porosities. In contrast, the analytical approximations derived here give very satisfactory agreement in all cases for both K and G.

[1]**email**: berryman@sep.stanford.edu
[2]Université de Rennes 1, Campus Beaulieu, Bât. 15, Rennes Cedex, France
email: spride@pangea.stanford.edu
[3]Dept. Geology and Geophysics, University of Wisconsin, Madison, Wisconsin
email: wang@geology.wisc.edu

INTRODUCTION

The elastic moduli of rock are dependent on its mineral properties, porosity distribution, and state of saturation. Two major theoretical approaches have been developed to address the problem of estimating elastic moduli from knowledge of rock constituents and microstructure. Effective medium theories, which include the classical bounds of Voigt (1928) and Reuss (1929) and Hashin and Shtrikman (1961,1962) as well as estimates obtained from self-consistent theories [*e.g.*, Hill (1965), Budiansky (1965), and Berryman (1980a,b)], require a parameter characterizing the pore distribution. Alternatively, poroelastic constitutive equations (Biot, 1941; Gassmann, 1951) are phenomenological and do not require characterization of matrix and pore space geometry. However, they contain the fundamental discrepancy that shear modulus is always independent of saturation state (Berryman, 1999). Although the lack of a shear dependence on saturating fluid bulk modulus can be correct for special microgeometries and very low modulation frequencies, this predicted lack of dependence is often contradicted by high frequency experiments (above ~ 1 kHz), and especially so in rocks with crack porosity. As a result, Biot's theory has been modified in various ways. For example, Mavko and Jizba (1991) partition porosity into "soft" and "stiff" porosity fractions to account for the change of both bulk modulus and shear modulus with fluid saturation.

Recent comprehensive reviews of the literature on analysis of cracked elastic materials include Kachanov (1992), Nemat-Nasser *et al.* (1993), and Kushch and Sangani (2000), as well as the textbook by Nemat-Nasser and Hori (1993). Some of the notable work on dry cracked solids using techniques similar to those that will be employed here includes Zimmerman (1985), Laws and Dvorak (1987), Hashin (1988), and Sayers and Kachanov (1991). Pertinent prior work on both dry and saturated cracked rocks includes Walsh (1969), Budiansky and O'Connell (1976), O'Connell and Budiansky (1974, 1977), Henyey and Pomphrey (1982), Hudson (1981, 1986, 1990), and Mavko and Jizba (1991).

The purpose of this paper is to obtain approximate analytical results for the elastic moduli of dry and fully-saturated cracked rock based on Differential Effective Medium (DEM) theory (Bruggeman, 1935; Cleary *et al.*, 1980; Walsh, 1980; Norris, 1985; Avellaneda, 1987). Penny-shaped cracks have been used extensively to model cracked materials (Walsh, 1969; Willis, 1980; Kachanov, 1992; Smyshlyaev *et al.*, 1993), but the penny-shaped crack model is itself an approximation to Eshelby's results (Eshelby, 1957; Wu, 1966) for oblate spheroids having small aspect ratio. In order to obtain some analytical formulas that are then relatively easy to analyze, a further simplifying assumption is made here that certain variations in Poisson's ratio with change of crack porosity can be neglected to first order. The consequences of this new approximation are checked by comparison with numerical computations for the fully coupled equations of DEM. The agreement between the analytical approximation and the full DEM for cracked rock is found to be quite good over the whole range of computed porosities. Justification for the approximation is provided in part by an analysis of the actual variation of Poisson's ratio and some further technical justifications are also provided in two appendices.

For simplicity, the main text of the paper treats materials having only crack porosity, and we consider these models to be granite-like idealizations of rock. A third appendix shows how the results of the main text change if the model is treated instead as a sandstone-like material

having finite stiff porosity in addition to the soft, crack porosity.

DIFFERENTIAL EFFECTIVE MEDIUM THEORY

Differential effective medium theory (Bruggeman, 1935; Cleary *et al.*, 1980; Walsh, 1980; Norris, 1985; Avellaneda, 1987) takes the point of view that a composite material may be constructed by making infinitesimal changes in an already existing composite. There are only two schemes known at present that are realizable, *i.e.*, that have a definite microgeometry associated with the modeling scheme. The differential scheme is one of these (Norris, 1985; Avellaneda, 1987). This fact provides a strong motivation to study the predictions of this theory because we can have confidence that the results will always satisfy physical and mathematical constraints, such as the Hashin-Shtrikman bounds (Hashin and Shtrikman, 1961; 1962).

When inclusions are sufficiently sparse that they do not form a single connected network throughout the composite, it is appropriate to use the Differential Effective Medium (DEM) to model their elastic behavior (Berge *et al.*, 1993). If the effective bulk and shear constants of the composite are $K^*(y)$ and $G^*(y)$ when the volume fraction of the inclusion phase is y, then the equations governing the changes in these constants are

$$(1-y)\frac{dK^*(y)}{dy} = \left[K_i - K^*(y)\right] P^{*i} \tag{1}$$

and

$$(1-y)\frac{dG^*(y)}{dy} = \left[G_i - G^*(y)\right] Q^{*i}, \tag{2}$$

where y is also porosity in the present case and the subscript i stands for inclusion phase. These equations are typically integrated starting from porosity $y = 0$ with values $K^*(0) = K_m$ and $G^*(0) = G_m$, which are assumed here to be the mineral values for the single homogeneous solid constituent. Integration then proceeds from $y = 0$ to the desired highest value $y = \phi$, or possibly over the whole range to $y = 1$. When integrating this way, we imagine the result is simulating cracks being introduced slowly into a granite-like solid. The same procedure can be used for a sandstone-like material assuming this medium has starting porosity $y = \phi_0$ with $K^*(\phi_0) = K_s$ and $G^*(\phi_0) = G_s$. Integration then proceeds from $y = \phi_0$ to $y = 1$. This introduction of crack (or soft) porosity into a material containing spherical (or stiff) porosity is conceptually equivalent to the porosity distribution model of Mavko and Jizba (1991). For simplicity, we will treat the granite-like case here, but the changes needed for other applications are not difficult to implement, and are treated specifically in Appendix A.

The factors P^{*i} and Q^{*i} appearing in (1) and (2) are the so-called polarization factors for bulk and shear modulus. These depend in general on the bulk and shear moduli of both the inclusion, the host medium (assumed to be the existing composite medium $*$ in DEM), and on the shapes of the inclusions. The polarization factors have usually been computed from Eshelby's well-known results (Eshelby, 1957) for ellipsoids, and Wu's work (Wu, 1966) on identifying the isotropically averaged tensor based on Eshelby's formulas. These results can be found in many places including Berryman (1980b, 1995) and Mavko *et al.* (1998).

The special case of most interest to us here is that for penny-shaped cracks, where

$$P^{*i} = \frac{K^* + \frac{4}{3}G_i}{K_i + \frac{4}{3}G_i + \pi\alpha\gamma^*} \tag{3}$$

and

$$Q^{*i} = \frac{1}{5}\left[1 + \frac{8G^*}{4G_i + \pi\alpha(G^* + 2\gamma^*)} + 2\frac{K_i + \frac{2}{3}(G_i + G^*)}{K_i + \frac{4}{3}G_i + \pi\alpha\gamma^*}\right], \tag{4}$$

with α being the crack (oblate spheroidal) aspect ratio, $\gamma^* = G^*[(3K^* + G^*)/(3K^* + 4G^*)]$, and where the superscript $*$ identifies constants of the matrix material when the inclusion volume fraction is y. This formula is a special limit of Eshelby's results not included in Wu's paper, but apparently first obtained by Walsh (1969). Walsh's derivation assumes that $K_i/K_m << 1$ and $G_i/G_m << 1$, and makes these approximations before making assumptions about smallness of the aspect ratio α. By taking these approximations in the opposite order, *i.e.*, letting aspect ratio be small first and then making assumptions about smallness of the inclusion constants, we would obtain instead the commonly used approximation for disks. But this latter approximation is actually inappropriate for the bulk modulus when the inclusion phase is air or gas (for then the ratio $K_i/K_m << 1$) or for the shear modulus when the inclusion phase is any fluid (for then $G_i \equiv 0$), as the formulas become singular in these limits. This is why the penny-shaped crack model is commonly used instead for rocks.

In general the DEM equations (1) and (2) are coupled, as both equations depend on both the bulk and shear modulus of the composite. This coupling is not a serious problem for numerical integration, and we will show results obtained from integrating the DEM equations numerically later in the paper. But, the coupling is a problem in some cases if we want analytical results to aid our intuition. We will now present several analytical results for both bulk and shear modulus, and then compare these results to the fully integrated DEM results later on.

Some analytical results for K^*

We now assume the inclusion phase is a fluid so $K_i = K_f$ and $G_i = G_f = 0$. The fluid can be either a liquid or a gas. We consider three cases: (1) liquid inclusion: $K_f >> \pi\alpha\gamma_m$, (2) gas inclusion: $K_f << \pi\alpha\gamma_m$, (3) general inclusion: $K_f \simeq \pi\alpha\gamma_m$. Case 1 corresponds to liquid inclusions, Case 2 to gas inclusions, and Case 3 to a circumstance in which crack aspect ratio is tuned to fluid modulus, or in which we do not want to limit ourselves to the assumptions of either of the previous two cases.

Liquid inclusion: $K_f >> \pi\alpha\gamma_m$

In this limit, it is somewhat more convenient to rewrite the DEM equations in terms of compliances, rather than stiffnesses, so we have

$$(1-y)\frac{d}{dy}\left(\frac{1}{K^*(y)}\right) = \left[K^*(y) - K_f\right]P^{*f}/(K^*)^2 = \left(\frac{1}{K_f} - \frac{1}{K^*}\right). \tag{5}$$

The only terms that couple the equations for bulk to shear have been readily neglected in this case, since $P^{*i} \simeq K^*/K_f$. Thus, we expect little if any deviation between the analytical results and the full DEM for the liquid saturated case. We are treating here the granite-like case such that the limit of zero inclusion volume fraction corresponds to $K^*(0) = K_m$, *i.e.*, the bulk modulus of the pure solid. Then, integrating (5) from $y = 0$ to $y = \phi$ (ϕ is the resulting porosity in the composite medium) gives directly

$$\left(\frac{1}{K_f} - \frac{1}{K^*}\right) = \left(\frac{1}{K_f} - \frac{1}{K_m}\right)(1-\phi). \tag{6}$$

which may be rearranged as

$$\left(\frac{1}{K^*} - \frac{1}{K_m}\right) = \left(\frac{1}{K_f} - \frac{1}{K_m}\right)\phi. \tag{7}$$

Eqn. (7) can also be obtained as the small ϕ limit of Gassmann's equation when the saturating fluid is a liquid. Gassmann's result for the bulk modulus (Gassmann, 1951) is expressible as

$$\frac{1}{K^*} = \frac{1-\theta B}{K_{dry}}, \tag{8}$$

where $\theta = 1 - K_{dry}/K_m$ is the Biot-Willis parameter (Biot and Willis, 1957), and B is Skempton's coefficient (Skempton, 1954)

$$B = \frac{\theta/K_{dry}}{\theta/K_{dry} + \phi(1/K_f - 1/K_m)}. \tag{9}$$

Expanding (8) for small ϕ gives (7) to first order in ϕ. Note however that Gassmann's full equation (8) has the further advantage that it is valid for all values of K_f (right down to zero), not just for values in the liquid range.

Eqn. (7) is also the result of Mavko and Jizba (1991) for a granite-like material under high confining pressure so that the crack-like pores are closed. Their result is stated for a sandstone-like material including both crack-like pores and other pores. But since we have not considered the presence of any other pores except the crack-like pores in this argument, the correct comparison material is just the mineral matrix.

Appendix A shows how to obtain the result of Mavko and Jizba (1991) from a modified DEM scheme.

Gas inclusion: $K_f << \pi\alpha\gamma_m$

For this limit, the stiffness form and the compliance form of the DEM equations are of equal difficulty to integrate, but a complication arises due to the presence of shear modulus dependence in the term γ_m in P. We are going to make an approximation (only for analytical calculations) that $\gamma^* \simeq K^*[3(1-2\nu_m)/4(1-\nu_m^2)]$, so the effect of variations in Poisson's ratio

away from ν_m for the matrix material is assumed *not* to affect the results significantly (*i.e.*, to first order) over the range of integration. Without this assumption, the DEM equations for bulk and shear are coupled and must be solved simultaneously (and therefore numerically in most cases).

With this approximation, the equation to be integrated then becomes

$$(1-y)\frac{dK^*(y)}{dy} = \frac{1}{b}\left[K_f - K^*(y)\right], \tag{10}$$

where

$$b = \frac{3\pi\alpha(1-2\nu_m)}{4(1-\nu_m^2)}. \tag{11}$$

The result of the integration is

$$K^* - K_f = (K_m - K_f)(1-\phi)^{\frac{1}{b}}. \tag{12}$$

This result seems to show a very strong dependence of K^* on the aspect ratio and Poisson's ratio through the product $\alpha(1-2\nu)$. But, we show in Appendix B that $\nu \to \nu_c \simeq \pi\alpha/18$, so only the dependence on α is significant.

It seems that this decoupling approximation might have a large effect for a dry system, but an exact decoupling can be achieved in this case (see Appendix B). The result shows that the only significant approximation we have made in (11) is one of order $2(\nu_c - \nu_m)$ and this term is of the order of 20% of b, and usually much less, for all the cases considered here.

General inclusion: K_f and $\pi\alpha\gamma_m$ arbitrary

Making the same approximations as in the previous case for γ_m, but making no assumption about the relative size of K_f and the aspect ratio, we find that DEM gives

$$\left(\frac{K^* - K_f}{K_m - K_f}\right)\left(\frac{K_m}{K^*}\right)^{\frac{1}{1+b}} = (1-\phi)^{\frac{1}{1+b}}, \tag{13}$$

which can be rewritten in the form

$$\left(\frac{1}{K_f} - \frac{1}{K^*}\right)\left(\frac{K^*}{K_m}\right)^{\frac{b}{1+b}} = \left(\frac{1}{K_f} - \frac{1}{K_m}\right)(1-\phi)^{\frac{1}{1+b}}. \tag{14}$$

It is now easy to check that (14) reduces to (6) when $b \to 0$ and that (14) reduces to (12) when $K_f \to 0$.

Analytical results for G^*

We now consider the same three cases for application of DEM to estimating the shear modulus G^*.

Liquid inclusion: $K_f >> \pi\alpha\gamma_m$

In this limit, the polarization factor for shear is given by

$$Q^{*f} \simeq \frac{1}{c} + \frac{4G^*}{15K_f}, \tag{15}$$

where

$$\frac{1}{c} \equiv \frac{1}{5}\left[3 + \frac{8(1-\nu_m)}{\pi\alpha(2-\nu_m)}\right]. \tag{16}$$

In this case, we have approximated $\gamma^* \simeq G^*/2(1-\nu_m)$ in order to decouple the G^* equation from the one for bulk modulus K^*. Note that as $y \to 1$, we anticipate $\nu^* \to 0.5$, so for ν^* in the usual range from 0 to 0.5 the factor $(1-\nu)$ varies at most by a factor of 2. Therefore, the condition on K_f is not affected. The parameter c depends on a factor $(1-\nu)/(2-\nu)$ which changes at most by a factor of $3/2$. Thus, we expect some small deviations between the analytical formula and the full DEM for G^* in the liquid saturated case.

Also note that we could argue, in this limit, that the first term on the right hand side of (15) is dominant and therefore the second term should be neglected. However, for purposes of comparison with Mavko and Jizba (1991), it will prove helpful to retain the second term.

Integrating the DEM equation, we have

$$\frac{1}{G^*} + \frac{4c}{15K_f} = \left(\frac{1}{G_m} + \frac{4c}{15K_f}\right)(1-\phi)^{-\frac{1}{c}}. \tag{17}$$

In the limit of small c (*i.e.*, small α) and $\phi \to 0$, we have

$$\frac{1}{G^*} - \frac{1}{G_m} = \left(\frac{4}{15K_f} + \frac{1}{cG_m}\right)\phi + \ldots, \tag{18}$$

which should be contrasted with the result of Mavko and Jizba [1991] for the same problem

$$\frac{1}{G^*} - \frac{1}{G_{dry}} = \frac{4}{15}\left(\frac{1}{K^*} - \frac{1}{K_{dry}}\right). \tag{19}$$

Because we need some other results to permit the analysis to proceed, a thorough comparison of the present results with the Mavko and Jizba formula will be postponed to the section on the ratio of compliance differences.

Gas inclusion: $K_f << \pi\alpha\gamma_m$

In this second limit, the equation for G^* is especially simple, since

$$Q^{*f} = \frac{1}{5}\left[1 + \frac{8(1-\nu_m)(5-\nu_m)}{3\pi\alpha(2-\nu_m)}\right] \equiv \frac{1}{d} \tag{20}$$

is a constant under our constant Poisson's ratio approximation. The DEM equation is then integrated to obtain

$$G^* = G_m(1-\phi)^{\frac{1}{d}} \tag{21}$$

which should be compared to (12). Within the analytical approximation, we will use (21) as our defining equation for G_{dry}, and note that we can then replace the volume fraction factor $1-\phi$ by

$$(1-\phi) = \left(\frac{G_{dry}}{G_m}\right)^d \tag{22}$$

whenever it is convenient to do so.

Our decoupling approximation for shear modulus in this case turns out to be somewhat better than the corresponding one for the bulk modulus. The result in Appendix B shows that the only significant approximation we have made in (20) is one of order $0.7(\nu_c - \nu_m)$ and this term is of the order of 7% of d or less for all the cases considered here. The relative error is therefore about one third of that made in the case of the bulk modulus.

General inclusion: K_f and $\pi\alpha\gamma_m$ arbitrary

In this more general case, we have

$$Q^{*f} = \frac{1}{c} + \frac{2G^*(2-3g)}{15(K_f + gG^*)}, \tag{23}$$

where

$$g \equiv \frac{\pi\alpha}{2(1-\nu_m)}. \tag{24}$$

Again, the DEM equations can be easily integrated and yield

$$\left(\frac{G^*}{G_m}\right)\left(\frac{\frac{1}{G^*} + \frac{cg}{dK_f}}{\frac{1}{G_m} + \frac{cg}{dK_f}}\right)^{1-\frac{c}{d}} = (1-\phi)^{\frac{1}{d}}. \tag{25}$$

Then, it is easy to check that the two previous cases are obtained when $\alpha \to 0$ and $K_f \to 0$, respectively.

EXAMPLES

We now consider some applications of these formulas. We take quartz as the host medium, having $K_m = 37.0$ GPa and $G_m = 44.0$ GPa. Poisson's ratio is then found to be $\nu_m = 0.074$.

For liquid saturation, the shear modulus goes to zero as the crack volume fraction increases, while the bulk modulus approaches the bulk modulus of the saturating liquid, which we take as water here ($K_f = 2.2$ GPa). This means that the effective value of Poisson's ratio increases towards $\nu^* = 0.5$ as the crack volume fraction increases, and thus the approximation that ν^* is constant clearly does not hold for this case. We therefore expect that the greatest deviations of the analytical approximation should occur for the case of liquid saturation.

In contrast, for the dry case, both shear modulus and bulk modulus tend towards zero as the crack volume fraction increases. Thus, since the trends for both moduli are similar, the approximation of constant Poisson ratio might hold in some cases, depending whether bulk and shear moduli go to zero at similar or very different rates with increasing crack volume fraction.

We consider three cases in Figures 1–6: (1) $\alpha = 0.1$ for Figures 1 and 2. (2) $\alpha = 0.01$ for Figures 3 and 4. (3) $\alpha = 0.001$ for Figures 5 and 6. The first two cases are easily integrated for DEM. We use two Runge-Kutta schemes from Hildebrand (1956): equations (6.13.15) and (6.14.5). When these two schemes give similar results to graphical accuracy, we can be confident that the step size used is small enough. If they differ or if either of them does not converge over the range of crack volume fractions of interest, then it is necessary to choose a smaller step size for integration steps. We found that a step size of $\Delta y = 0.01$ was sufficiently small for both $\alpha = 0.1$ and $\alpha = 0.01$, while it was necessary to decrease this step size to $\Delta y = 0.001$ for the third case, $\alpha = 0.001$. (Still smaller steps were used in some of the calculations to be described later.)

The results show that our expectations for the agreement between the analytical and numerical results are in concert with the results actually obtained in all cases. The analytical approximation gives a remarkably good estimate of the numerical results in nearly all cases, with the largest deviations occurring — as anticipated — for the intermediate values of crack volume fraction in the cases of liquid saturation for the bulk modulus estimates. We consider that the results of Figures 1–6 are in sufficiently good agreement that they provide cross-validation of both the numerical and the analytical methods.

For the saturated case, we anticipated little if any deviation for the bulk modulus between the analytical results and the full DEM as is observed for $\alpha = 0.1$ and $\alpha = 0.01$. Larger deviations are found for $\alpha = 0.001$. We also observed the anticipated small deviations for the shear modulus between the analytical formula and the full DEM.

Note that Gassmann's predictions for bulk modulus are in very good agreement with the numerical DEM results for saturated cracks and $\alpha = 0.001$.

For the dry case, we anticipated that the analytical shear modulus formula would be a somewhat better approximation of the full DEM, than that for the bulk modulus. Both approximations were expected to be quite good. These results are also observed in the Figures.

On improvements

The analytical results obtained here for the dry case could be improved somewhat several different ways. Instead of replacing ν^* by ν_m, we could have replaced it by the fixed point value ν_c obtained in Appendix B. Since the fixed point is an attractor and the values rapidly approach ν_c for small but finite volume fractions, this approximation would guarantee an improved approximation over most of the range of crack volume fraction. However, it will make the approximation a little worse in the very small volume fraction region. It has been and will continue to be a significant advantage for our analysis to have formulas valid in the small ϕ limit, so we have chosen not to do this here. Alternatively, instead of choosing either of the extreme values of ν^*, we could use their mean, their harmonic mean, or their geometric mean, etc., with similar benefits and drawbacks. Or, we could make direct use of the results from Appendix B for the decoupled equation for Poisson's ratio. This approach will improve the results over the whole range of volume fractions, but will complicate the formulas considerably. We want to emphasize, however, that our goal here has not been to achieve high accuracy in the analytical approximation, but rather to gain insight into what the equations were computing and why. Having accomplished this even with the simplest approximation $\nu^* \simeq \nu_m$, we do not think it fruitful to dwell on this issue and we will therefore leave this part of the subject for now. For the interested reader, some additional technical justifications of the analytical approximation are provided in Appendix C.

Next we want to do more detailed comparisons between these results and those of Gassmann (1951) and of Mavko and Jizba (1991) in the remainder of the paper.

RATIO OF COMPLIANCE DIFFERENCES

We have already seen that there are several advantages of the differential scheme presented here for purposes of analysis. Another advantage will soon become apparent when we analyze the ratio of the compliance differences

$$R = \frac{1/G^* - 1/G_{dry}}{1/K^* - 1/K_{dry}}. \tag{26}$$

This ratio is of both theoretical and practical interest. It is of practical interest because it is often easier to measure bulk moduli, and it would therefore be possible to estimate the shear behavior from the bulk behavior if the ratio R were known to be either a universal constant, or a predictable parameter. Mavko and Jizba (1991) show that this ratio is given by $R \simeq 4/15$ when the differences between the dry and the starred quantities are due to a small amount of soft (crack-like) porosity that is liquid filled for the starred moduli. The derivation of this ratio makes it clear that the value $R = 4/15$ is actually an upper bound, *i.e.*, a value that cannot be exceeded for such systems, but also a value that clearly is not achieved for many systems lacking such soft porosity. In particular, it was already known by Mavko and Jizba (1991) that $R \simeq 0$ when the microgeometry of all the porosity is spherical. The crack-like porosity in Mavko and Jizba's model has finite compressiblity normal to its plane and is incompressible in the plane of the crack. Thus, their soft porosity can be thought of as cracks whose aspect

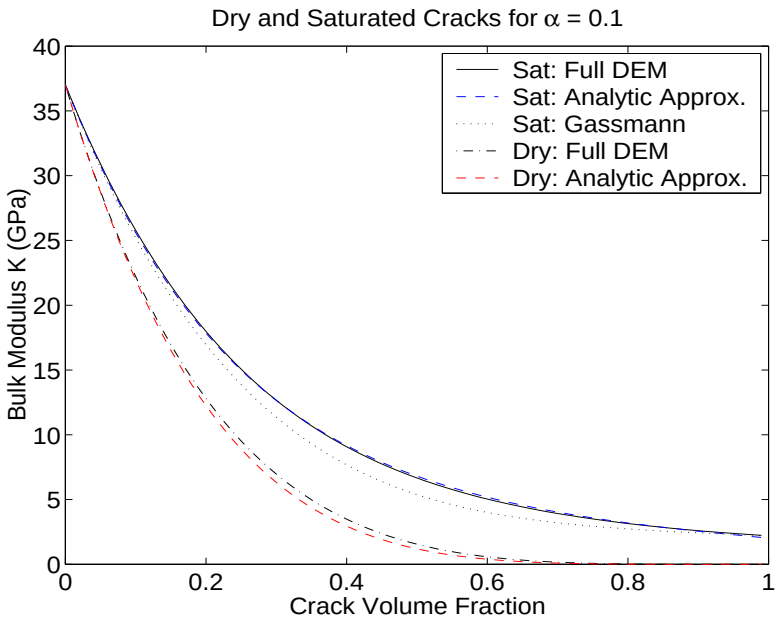

Figure 1: Bulk modulus for dry and liquid saturated cracked porous media with $\alpha = 0.1$. Full DEM calculation is shown as a solid line for the saturated case and as a dot-dash line for the dry case. The analytical approximations in the text are displayed as a dashed line for both dry and saturated cases. Agreement between full DEM and analytical approximation is excellent in both cases. Gassmann's prediction is shown by the dotted line. jim1-allk1pg [NR]

ratios approach zero. Goertz and Knight (1998) have also done a parameter study showing that a related ratio (RG_m/K_m) is generally less than $4/15$ for oblate spheroids and it tends to zero as the oblate spheroids' aspect ratios approach unity. It would be helpful to see this behavior directly in the equations, and it is the purpose of this section to show this behavior analytically.

Each of the four material constants appearing in (26) can be computed/estimated using the DEM. But, R is normally defined only in the limit of very small values of soft porosity, in which case both the numerator and the denominator tend to zero. This type of limit is well-known in elementary calculus, and the result is given by L'Hôpital's rule:

$$R = \frac{d(1/G^* - 1/G_{dry})/dy}{d(1/K^* - 1/K_{dry})/dy}. \tag{27}$$

From this form of R, it is now quite easy to relate the ratio to the P's and Q's discussed earlier. In particular, we find that

$$(1-y)\frac{d}{dy}(1/G^* - 1/G_{dry}) = \frac{2K_f}{5G_m}\frac{\pi\alpha\gamma_m - 2G_m/3}{\pi\alpha\gamma_m(K_f + \pi\alpha\gamma_m)} \tag{28}$$

and

$$(1-y)\frac{d}{dy}(1/K^* - 1/K_{dry}) = -\frac{K_f}{\pi\alpha\gamma_m(K_f + \pi\alpha\gamma_m)}\left(1 + 3\pi\alpha(1-2\nu_m)/4(1-\nu_m^2)\right), \tag{29}$$

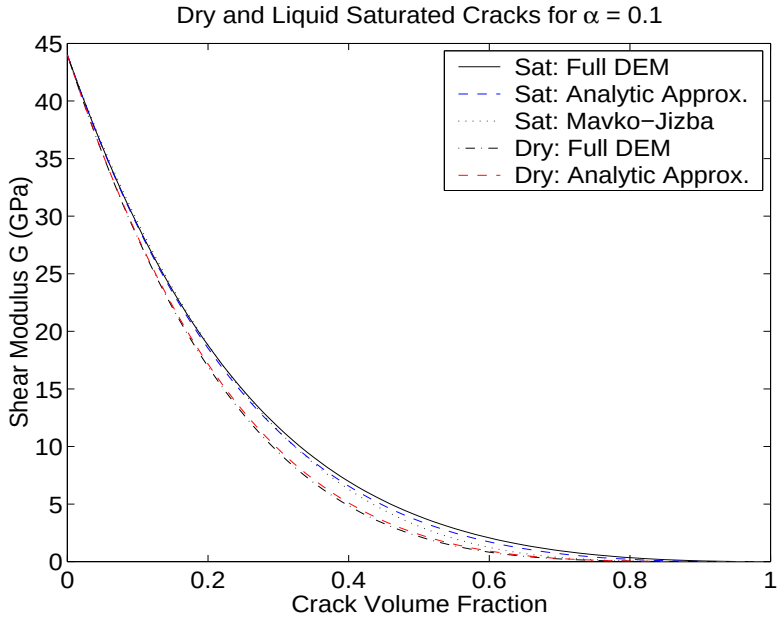

Figure 2: Shear modulus for dry and liquid saturated cracked porous media with $\alpha = 0.1$. Full DEM calculation is shown as a solid line for the saturated case and as a dot-dash line for the dry case. The analytical approximations in the text are displayed as a dashed line for both dry and saturated cases. Agreement between full DEM and analytical approximation is again excellent in both cases. The Mavko-Jizba (1991) prediction is shown by the dotted line. jim1-allmu1pmj [NR]

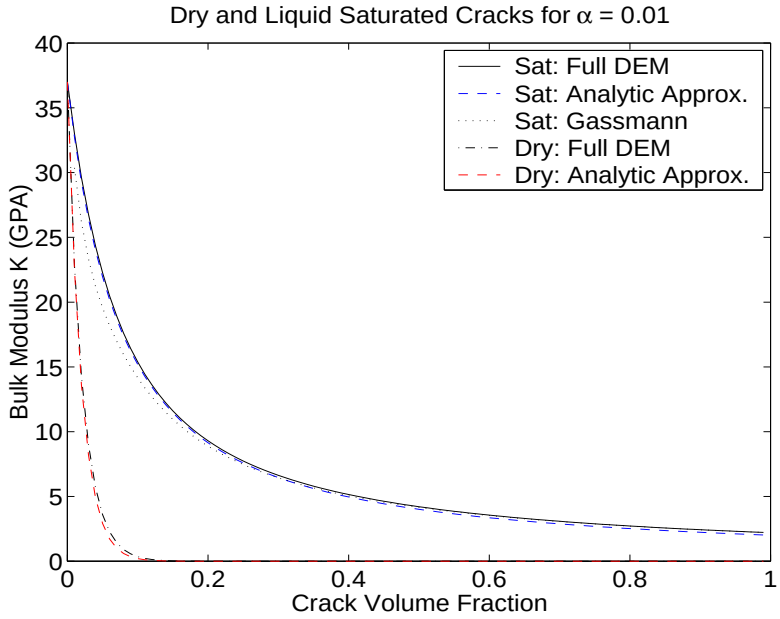

Figure 3: Same as Figure 1 for $\alpha = 0.01$. jim1-allk01pg [NR]

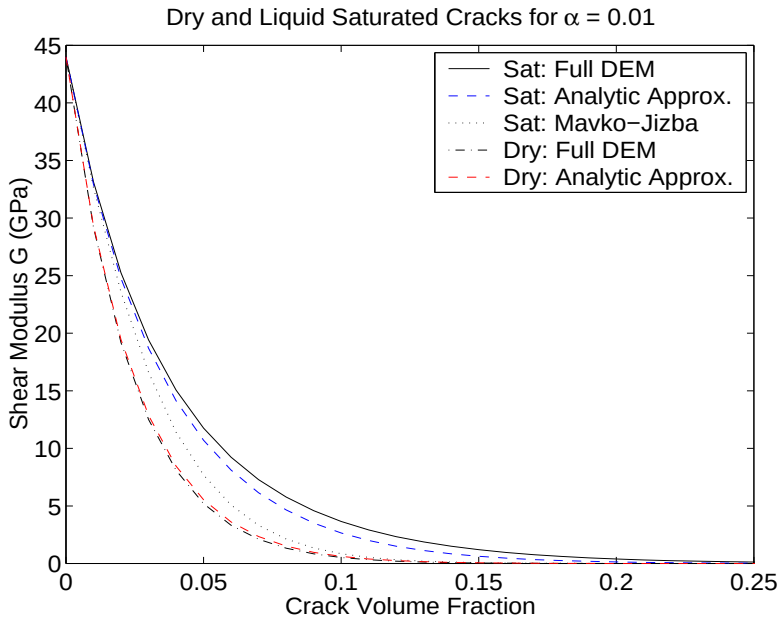

Figure 4: Same as Figure 2 for $\alpha = 0.01$. Note that the Mavko-Jizba agreement is poor except at low porosities ($<\sim$ 2%). jim1-allmu01pmj_25 [NR]

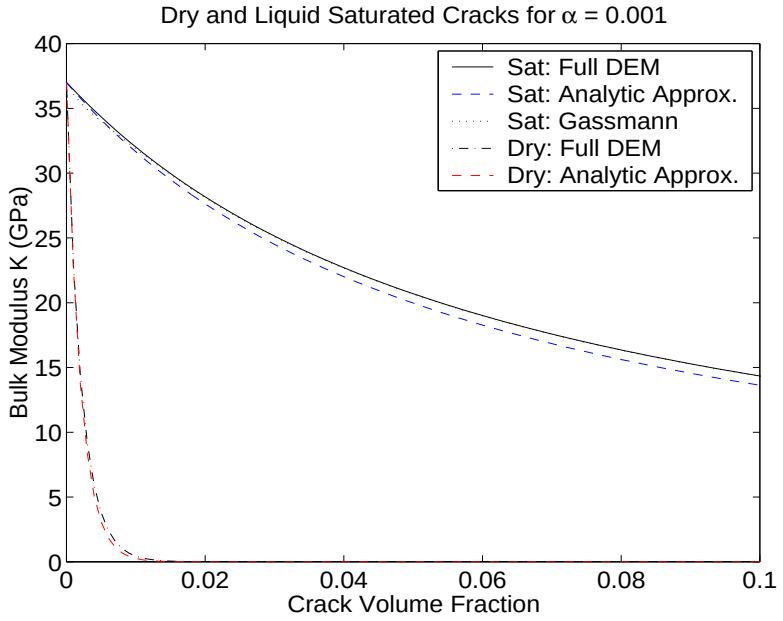

Figure 5: Same as Figure 1 for $\alpha = 0.001$. Gassmann (1951) is in very good agreement with DEM for this case. jim1-allk001pg_0.1 [NR]

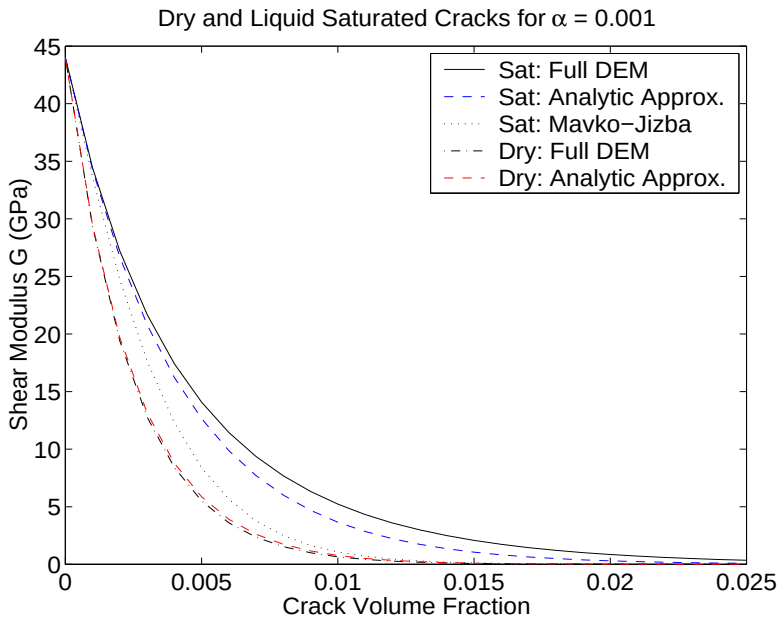

Figure 6: Same as Figure 2 for $\alpha = 0.001$. Again, note that the Mavko-Jizba prediction is in poor agreement except at very low porosities ($<\sim 0.2\%$). jim1-allmu001pmj [NR]

and therefore that

$$R = \frac{4}{15}\left(1 - \frac{3\pi\alpha}{4(1-\nu_m)}\right)\left(1 + 3\pi\alpha(1-2\nu_m)/4(1-\nu_m^2)\right)^{-1}. \tag{30}$$

[For sandstones, we could instead evaluate (30) at $y = \phi_0$ and $\nu(\phi_0) = \nu_s$. It is only the soft, crack-like porosity that needs to be very small for (30) to be applicable.] Equation (30) is an exact expression for the ratios of these two slopes when the calculation starts at $y = 0$ and $\nu(0) = \nu_m$. It depends only on the aspect ratio α and Poisson's ratio ν_m of the mineral. It shows a sublinear decrease of R with increasing α, and the value of R reaches zero when $\alpha_c = 4(1-\nu_m)/3\pi$. Because the formulas used for the penny-shaped crack model are valid only for very low aspect ratios, this latter behavior should not be taken literally. We do expect R to decrease as the aspect ratio increases, and the trend should be to zero, but this zero value should only be achieved at $\alpha = 1$. This is the type of behavior observed, for example, by Goertz and Knight (1998). We will check the quantitative predictions by doing a numerical study here for oblate spheroids as a function of aspect ratio. The results will be similar to those obtained by Goertz and Knight (1998), but not identical for several reasons: (1) Goertz and Knight plot RG_m/K_m (instead of R) for the Mori-Tanaka method (Benveniste, 1987), (2) the R values presented here are for an infinitesimal change in soft porosity, and (3) the present calculation is (therefore) actually not dependent on the type of effecive medium approximation used, only on the Eshelby (1957) and Wu (1966) factors P and Q.

The appropriate expressions for P and Q for oblate spheroids can be found in Berryman (1980b). We repeat the analysis given above in (27)–(29) step by step for oblate spheroids. The results are shown in Figure 7, together with the results obtained using the penny-shaped

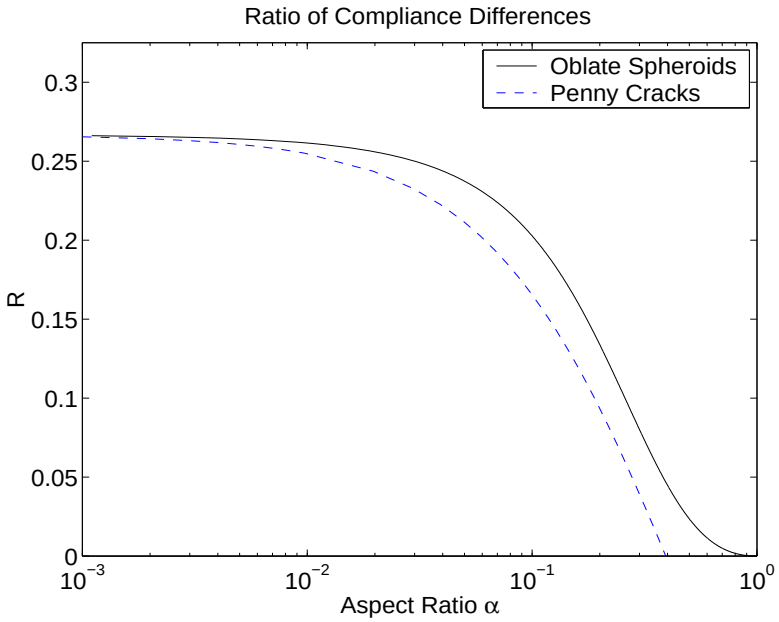

Figure 7: Ratio of compliance differences R as a function of aspect ratio for oblate spheroids and for the penny-shaped crack approximation to oblate spheroids. Note that the asymptotic value for small α is $R = 4/15$ in both cases, in agreeement with Mavko and Jizba (1991). jim1-Rratio_log [NR]

cracks as presented already in Equation (30). We see that the results agree completely for α's smaller than about 0.001, and are in qualitative agreement over most of the rest of the range. As already discussed, the penny-shaped crack model is a limiting approximation for the oblate spheroids, and deviations from the curve for oblate spheroids do not have physical significance; they merely indicate the degree of error inherent in this choice of approximation scheme. The results for oblate spheroids should be considered rigorous.

DISCUSSION AND CONCLUSIONS

Discussion

We began the paper by pursuing the differential effective medium predictions for the bulk and shear moduli in a cracked material in which the cracks can be either gas-saturated (dry) or liquid-saturated. The DEM equations can be integrated numerically without serious difficulty for the exact model of oblate spheroids of arbitrary aspect ratio, but the full formulas for oblate spheroids are rather involved. In order to make progress on analytical expressions, part of the effort was directed towards study of the penny-shaped crack model of Walsh (1969). This model is not too difficult to analyze if an additional approximation is entertained. The problem for analysis is that the ordinary differential equations for bulk and shear moduli are coupled. If they can be decoupled either rigorously or approximately, then they can be inte-

grated analytically. We accomplished the decoupling for the penny crack model by assuming that changes in Poisson's ratio occurring in those terms proportional to the aspect ratio are negligible to first order. This permits the decoupling to occur and the integration to proceed. We could subsequently check the analytical results against the full DEM integration for penny-shaped cracks, which showed that the analytical results were in quite good agreement with the numerical results.

To attempt to understand why the analytical results worked so well, we studied the behavior of Poisson's ratio for the same system, and found that, as the porosity increases, for the dry systems Poisson's ratio tends to a small positive value on the order of $\pi\alpha/18$, where α is the aspect ratio, and for liquid saturated systems it tends towards $1/2$ in all cases. These results permit error estimates for the analytical formulas showing that errors will always be less than about 5%–20%, depending on the aspect ratio and the porosity value.

We have also shown that the Mavko and Jizba (1991) proportionality factor of $4/15$ relating the differences in shear compliances to the differences in bulk compliances for cracked systems is an upper bound and that this upper bound is approximately achieved for $\alpha \leq 0.001$. The proportionality factor decreases monotonically with increasing aspect ratio of oblate spheroids, and vanishes identically for spheres at $\alpha = 1$.

Conclusions

The analytical approximation made in this paper seems to be very effective at capturing the first order behavior of the bulk and shear moduli for cracked porous media in both the dry and saturated cases. The resulting formulas are not rigorous, unlike Gassmann's formulas for low frequency behavior, but these approximate formulas nevertheless have a wider range of validity (considering both porosity and frequency ranges) than either Gassmann (1951) or Mavko and Jizba's (1991) results.

We believe these results will, at the very least, provide a helpful way of understanding the behavior of these complex systems, and may also provide a stepping stone towards more general formulas in the future.

APPENDIX A – SANDSTONE-LIKE SAMPLE CALCULATIONS

The main focus of the paper is on the effects of addition of cracks to pre-existing materials. When cracks are added to homogeneous background, we think of this as being a granite-like material. This case has been treated in the main text. To show the generality of the method, we want to give a brief treatment of the sandstone-like situation of a material having a pre-exisiting porosity ϕ_0 in this appendix. This porosity may itself be either liquid saturated or gas saturated (dry). For simplicity, we will assume here that ϕ_0 is liquid saturated when liquid saturated cracks are to be added, dry when dry cracks are to be added.

There are two further alternatives to be considered. First, cracks may be added randomly to the pre-existing material. Second, cracks may be added preferentially to the porosity-free

host material. We discuss these two cases in turn.

Random addition of cracks

Random addition of inclusions is the case considered in the main text, so the DEM equations themselves do not change. We use (1) and (2) as before, but the range of integration changes to the interval starting at $y = \phi_0$ up to $y = \phi = \phi_0 + \phi_{crack}$. The only differences in the resulting formulas are that (a) everywhere the factor $(1-\phi)$ appeared before it is now replaced by the ratio $(1-\phi)/(1-\phi_0)$, and (b) everywhere K_m and G_m appeared these material constants are replaced by $K(\phi_0)$ and $G(\phi_0)$. So, for example, equation (6) becomes

$$\frac{1}{K_f} - \frac{1}{K^*} = \left(\frac{1}{K_f} - \frac{1}{K(\phi_0)}\right)\left(\frac{1-\phi}{1-\phi_0}\right) \tag{31}$$

When $\phi_{crack} << (1-\phi_0)$, we can rewrite this expression as

$$\frac{1}{K^*} - \frac{1}{K(\phi_0)} = \left(\frac{1}{K_f} - \frac{1}{K(\phi_0)}\right)\left(\frac{\phi_{crack}}{1-\phi_0}\right) \tag{32}$$

This formula still differs from the Mavko and Jizba (1991) result, but the difference is nevertheless expected because their derivation does not assume random placement of cracks. We can resolve this discrepancy when we make use of an assumption of preferential addition of cracks in the next subsection.

Preferential addition of cracks

The factor $(1-y)$ on the left hand sides of both (1) and (2) arises from the need to account for the fact that, when an inclusion is placed in a composite, the volume of the inclusion replaces not only host material, but also some of the other inclusion material previously placed in the composite. When y is the inclusion volume fraction, the remaining host volume fraction is $(1-y)$. So random replacement of dy of the composite medium only replaces $(1-y)dy$ of the host material. Replacing instead $dy/(1-y)$ of the composite then gives the correct factor of dy host replacement; thus, the factor of $(1-y)$ is required in (1) and (2) for random inclusion placement at finite values of y.

If we now assume instead that the inclusions are place preferentially in pure host material (and this gets progressively harder to do in practice for larger integrated overall inclusions fractions y), then the DEM equations must be modified to account for this situation.

For example, with preferential addition of inclusions, it is clear from the preceding considerations that DEM equation (5) is replaced by

$$\frac{d}{dy}\left(\frac{1}{K^*}\right) \simeq \frac{1}{K_f} - \frac{1}{K_m}. \tag{33}$$

Integrating (33) gives

$$\frac{1}{K^*} - \frac{1}{K(\phi_0)} = \left(\frac{1}{K_f} - \frac{1}{K_m}\right)\phi_{crack}. \tag{34}$$

The validity of this result clearly depends on ϕ_0 being sufficiently small so that it is possible to find enough pure host material to which cracks can be added "randomly." Taking $\phi_0 \to 0$ guarantees satisfaction of the requirement, but the approximation must eventually break down as $\phi_0 \to 1$.

Eqn. (34) is almost the corresponding result of Mavko and Jizba (1991). Mavko and Jizba use as their comparison state the dry porous material, assuming that no cracks are present or that, when present, they are closed due to applied external pressure. We can also obtain the same result using (33), but now $K^*(\phi_0) = K_{dry}(\phi_0)$, so the integration has a different starting value than in the previous paragraph. Then, we find

$$\frac{1}{K^*_{MJ}} - \frac{1}{K_{dry}(\phi_0)} = \left(\frac{1}{K_f} - \frac{1}{K_m}\right)\phi_{crack}. \tag{35}$$

Eqn. (35) is exactly the corresponding result of Mavko and Jizba (1991). Although the right hand sides of (34) and (35) are identical, the results differ, *i.e.*, $K^* \neq K^*_{MJ}$, since the assumed host material is fluid saturated in the first case and dry in the second case.

APPENDIX B – POISSON'S RATIO FOR DRY CRACKS

When the cracks are taken to be dry, so that $K_i = G_i = 0$ in (1) and (2), it turns out that an elegant decoupling of the DEM equations is possible [also see Zimmerman (1985) and Hashin (1988)]. If we consider the parameter ratio $G^*/K^* = 3(1-2\nu^*)/2(1+\nu^*)$, we find that it satisfies the equation

$$(1-y)\frac{d\ln(G^*/K^*)}{dy} = -\frac{3(1-y)}{(1+\nu^*)(1-2\nu^*)}\frac{d\nu^*}{dy} = P^{*i} - Q^{*i}. \tag{36}$$

Furthermore, it is generally true for dry inclusions (not just for penny-shaped cracks) that both P^{*i} and Q^{*i} are functions only of the same ratio G^*/K^*, or equivalently of Poisson's ratio ν^*. Thus, we can solve (36) for either ν^* or the ratio of moduli, without considering any other equation.

It is also important to notice that the dimensionless polarization factors P and Q are both often close to unity, and furthermore that it is possible that, for special values of Poisson's ratio, we might find $P^{*i} = Q^{*i}$. If this happens for some critical value $\nu^* = \nu_c$, then the equation (36) guarantees that this value of Poisson's ratio will be preserved for all values of porosity, since the right hand side vanishes initially, and therefore always. Such a critical value is usually called a *fixed point* of the equations, and such fixed points can be either *stable* or *unstable*. If they are unstable, then a small deviation from the critical point causes a rapid divergence of Poisson's ratio from the fixed point. If they are stable, then a small deviation produces a situation in which the value of Poisson's ratio gradually (asymptotically) approaches the critical value. When this happens, we say the fixed point is an *attractor*. For the DEM equation (36), a fixed point that is an attractor will only be reached in the limit $\phi \to 1$, but the value of Poisson's ratio will change fairly rapidly in the direction of the attractor when the first cracks are added to the system. Such behavior of Poisson's ratio has been noted before by Zimmerman (1994) and by Dunn and Ledbetter (1995), among others.

For penny-shaped cracks, we have

$$P^{*i} - Q^{*i} = \frac{4(1-\nu^{*2})}{3\pi\alpha(1-2\nu^*)} - \frac{1}{5}\left[1 + \frac{8(1-\nu^*)(5-\nu^*)}{3\pi\alpha(2-\nu^*)}\right], \tag{37}$$

which has a fixed point approximately (using one step of a Newton-Raphson iteration scheme) at

$$\nu_c = \frac{2\pi\alpha}{36+5\pi\alpha}. \tag{38}$$

This shows that, when α is very small, Poisson's ratio for the dry cracked material tends toward small positive values. For somewhat larger values of α, Poisson's ratio approaches a value proportional to α and on the order of $\pi\alpha/18$.

For comparison, consider spherical void inclusions [see Berryman (1980) for the general expressions for P and Q]. Then, we have

$$P^{*i} - Q^{*i} = \frac{1+\nu^*}{2(1-2\nu^*)} - \frac{2(4-5\nu^*)}{7-5\nu^*}, \tag{39}$$

which has a fixed point at

$$\nu_c = \frac{1}{5}. \tag{40}$$

This result has been remarked upon previously by Zimmerman (1994). Similarly considering needle-shaped void inclusions, we have

$$P^{*i} - Q^{*i} = \frac{2(1+\nu^*)}{3(1-2\nu^*)} - \frac{1}{5}\left[\frac{7}{3} + 2(3-4\nu^*)\right], \tag{41}$$

which has a fixed point at

$$\nu_c = \frac{1}{8}\left[7 - \sqrt{29}\right] \simeq 0.20185. \tag{42}$$

Dunn and Ledbetter (1995) have shown that all the prolate spheroids have critical Poisson's ratios close to that for spheres. We see that needles, being the extreme case of prolate spheroids, is in agreement with this result.

Dunn and Ledbetter (1995) have shown that disk-shaped inclusions (which are achieved by taking oblate spheroids to the $\alpha = 0$ limit) have a critical Poisson's ratio of $\nu_c = 0$. This result and the others obtained above are collected for comparison in TABLE 1.

TABLE 1. Fixed points of equation (36) for commonly considered inclusion shapes.

Shape	ν_c
Needle	~ 0.202
Sphere	$\frac{1}{5}$
Penny	$\sim \frac{2\pi\alpha}{36+2.245\pi\alpha}$
Disk	0

TABLE 2. Typical values of Poisson's ratio for various solid materials contained in rocks. See for example Mavko *et al.* (1998).

Mineral	ν_m
Quartz	0.06 – 0.08
Corundum	0.24
Dolomite	0.20 – 0.30
Calcite	0.29 – 0.32
Feldspar	0.32 – 0.35

To clarify the behavior of the solution of (36), we will do an approximate analysis by expanding the right hand side around $\nu = 0$ and also note that for small ν, $G^*/K^* \simeq 3(1-3\nu^*)/2$. Then, (36) becomes

$$(1-y)\frac{d\nu^*}{dy} \simeq \frac{1}{15} - \frac{6\nu^*}{5\pi\alpha}, \tag{43}$$

which can easily be integrated to yield

$$(\frac{\pi\alpha}{18} - \nu^*) \simeq (\frac{\pi\alpha}{18} - \nu_m)(1-\phi)^{\frac{1}{h}} \tag{44}$$

where ν_m is the starting, or in our case the mineral, value of Poisson's ratio, and

$$h = 5\pi\alpha/6. \tag{45}$$

A more precise, and therefore more tedious, analysis of the right hand side of (37) gives the improved approximation (38) for the asymptotic value of ν_c.

In Figure 8, we show the actual results for Poisson's ratio from the full DEM in the same three examples shown in Figures 1–6. The starting value of Poisson's ratio is $\nu_m = 0.0742$. For comparison, TABLE 2 contains a listing of various Poisson's ratios for minerals that could be important in rocks in order to show the range of behavior observed in nature. Except for different starting locations, we expect the qualitative behavior of the curves for Poisson's ratio to closely follow that of Figure 8 and (44) in all cases.

[Technical note concerning the dry case: For $\alpha = 0.1$, the Runge-Kutta scheme used to solve the coupled DEM equations for K^* and G^* was sufficiently accurate that ν^* could be computed from these values. However, for $\alpha = 0.01$ and 0.001, the accuracy obtained was not sufficient, so we instead used the same Runge-Kutta scheme but applied it directly to (36). This approach gave very stable results.]

Figure 9 compares the results for oblate spheroids to those of penny-shaped cracks; both curves are obtained by finding the zeros of $P - Q$ numerically. To provide additional insight, the curve $\nu = \frac{2\pi\alpha}{36+2.245\pi\alpha}$ [which was obtained by using the functional form of (38) and fitting the coefficient in the denominator at $\alpha = 1$] is also shown. We see that the results for penny-shaped cracks deviate substantially from those of oblate spheroids as $\alpha \to 1$, but they are in agreement at lower values of $\alpha \leq 0.001$. The deviations from the results for oblate spheroids, again, are not physical and should simply be viewed as artifacts introduced by the very low aspect ratio limiting procedure used to obtain the approximate formulas for penny-shaped cracks.

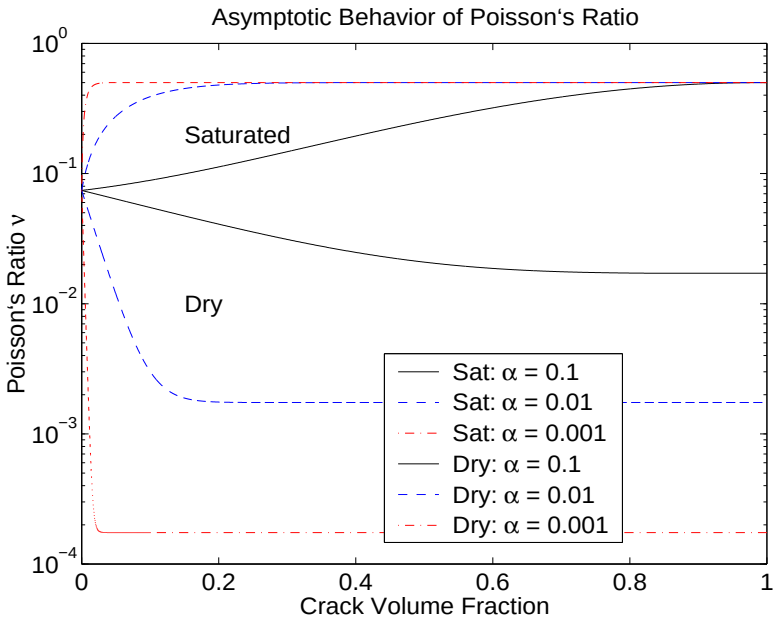

Figure 8: Asymptotic behavior of Poisson's ratio as a function of crack volume fraction for three values of α: 0.1, 0.01, 0.001. The asymptotic value for saturated samples is always $\nu_c = 1/2$. For dry samples, the asymptotic value depends on the geometry of the inclusion, and therefore on α for cracks. The limiting value $\nu_c \simeq \pi\alpha/18$ is a stable attractor of the DEM equations, as is observed in this figure. jim1-nu_long [NR]

APPENDIX C – TECHNICAL JUSTIFICATION OF THE APPROXIMATION FOR γ

It is inherent in the mathematical form of all DEM schemes that they always give correct values and slopes of the curves for small values of the inclusion volume fraction, and that they always give the right values (but not necessarily correct slopes) at high volume fractions. We see that these expectations are fulfilled in all the examples shown here.

The approximations made in the text to arrive at analytical results were chosen as a convenient means to decouple the equations for bulk and shear moduli, which are normally coupled in the DEM scheme. For the *liquid saturated* case, the approximations for bulk modulus are very good for all values of aspect ratio, but for shear modulus the exponent determined by (16) can deviate as much as a factor of $2/3$. The value chosen is the maximum value possible, guaranteeing that the analytical approximation will always be a lower bound for this case.

In contrast, for the case of *dry* cracks, the approximations for the shear modulus are expected to be somewhat better than those for the bulk modulus. The analytical approximation is again expected to be a lower bound for the full DEM result for the shear modulus. Analysis for the bulk modulus is more difficult in this limit as it requires checking that the ratio G^*/K^* remains finite as the porosity $\phi \to 1$, and this would be difficult to establish if Poisson's ratio were going to $\nu = 1/2$, as it does for the liquid saturated case. But, Appendix B shows that Poisson's ratio actually tends to a value of about $\nu_c \simeq \pi\alpha/18$, so there is no singularity in the

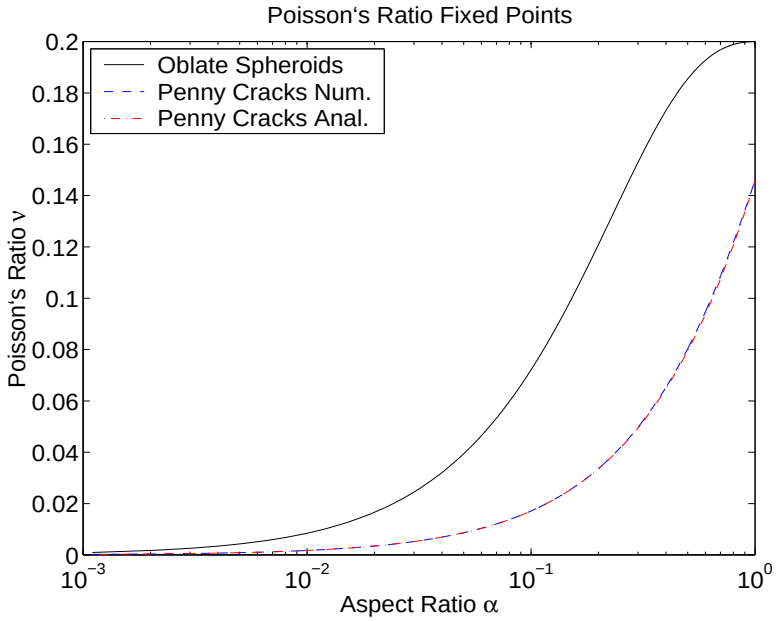

Figure 9: Poisson's ratio fixed point ν_c as a function of α found numerically for oblate spheroids and penny-shaped cracks, and also for penny-shaped cracks using the analytical expression $\nu_c = 2\pi\alpha/(36.0 + 2.245\pi\alpha)$. The two curves for penny-shaped cracks are nearly indistinguishable on the scale of this plot. The correct fixed point for spheres ($\alpha = 1$) is $\nu_c = 1/5$, and this value is attained in the $\alpha \to 1$ limit by the curve for oblate spheroids. jim1-Nuoblate_log [NR]

K^* behavior for this case. This feature is also confirmed by the numerical results.

ACKNOWLEDGMENTS

We thank Gary Mavko for a very helpful discussion of his own results regarding fluid effects on the shear modulus.

REFERENCES

Avellaneda, M., 1987, Iterated homogenization, differential effective medium theory and applications: *Commun. Pure Appl. Math* **40**, 527–554.

Benveniste, Y., 1987, A new approach to the application of Mori-Tanaka's theory in composite materials: *Mech. Mat. 6*, 147–157.

Berge, P. A., Berryman, J. G. & Bonner, B. P., 1993, Influence of microstructure on rock elastic properties: *Geophys. Res. Letters* **20**, 2619–2622.

Berryman, J. G., 1980a, Long-wavelength propagation in composite elastic media I. Spherical inclusions: *J. Acoust. Soc. Am.* **68**, 1809–1819.

Berryman, J. G., 1980b, Long-wavelength propagation in composite elastic media II. Ellipsoidal inclusions: *J. Acoust. Soc. Am.* **68**, 1820–1831.

Berryman, J. G., 1995, Mixture theories for rock properties: in *Rock Physics and Phase Relations*, edited by T. J. Ahrens, AGU, Washington, DC, pp. 205–228.

Berryman, J. G., 1999, Origin of Gassmann's equations: *Geophysics* **64**, 1627–1629.

Biot, M. A., 1941, General theory of three-dimensional consolidation: *J. Appl. Phys.* **12**, 155–164.

Biot, M. A. & Willis, D. G., 1957, The elastic coefficients of the theory of consolidation: *J. App. Mech.* **24**, 594–601.

Bruggeman, D. A. G., 1935, Berechnung verschiedener physikalischer Konstanten von heterogenen Substanzen: *Ann. Physik. (Leipzig)* **24**, 636–679.

Budiansky, B., 1965, On the elastic moduli of some heterogeneous materials: *J. Mech. Phys. Solids* **13**, 223–227.

Budiansky, B. & O'Connell, R. J., 1976, Elastic moduli of a cracked solid: *Int. J. Solids Struct.* **12**, 81–97.

Cleary, M. P, Chen, I.-W., & Lee, S.-M., 1980, Self-consistent techniques for heterogeneous media: *ASCE J. Eng. Mech.* **106**, 861–887.

Dunn, M. L., & Ledbetter, H., 1995, Poisson's ratio of porous amd microcracked solids: Theory and application to oxide superconductors: *J. Mater. Res.* **10**, 2715–2722.

Eshelby, J. D., 1957, The determination of the elastic field of an ellipsoidal inclusion, and related problems: *Proc. Roy. Soc. London A* **241**, 376–396.

Gassmann, F., 1951, Über die elastizität poröser medien: *Veirteljahrsschrift der Naturforschenden Gesellschaft in Zürich* **96**, 1–23.

Goertz, D., & Knight, R., 1998, Elastic wave velocities during evaporative drying: *Geophysics* **63**, 171–183.

Hashin, Z., 1988, The differential scheme and its application to cracked materials: *J. Mech. Phys. Solids* **36**, 719–734.

Hashin, Z., & Shtrikman, S., 1961, Note on a variational approach to the theory of composite elastic materials: *J. Franklin Inst.* **271**, 336–341.

Hashin, Z. & Shtrikman, S., 1962, A variational approach to the theory of elastic behaviour of polycrystals: *J. Mech. Phys. Solids* **10**, 343–352.

Henyey, F. S., & Pomphrey, N., 1982, Self-consistent elastic moduli of a cracked solid: *Geophys. Res. Lett.* **9**, 903–906.

Hildebrand, F. B., 1956, *Introduction to Numerical Analysis*, Dover, New York, pp. 285–297.

Hill, R., 1965, A self-consistent mechanics of composite materials: *J. Mech. Phys. Solids* **13**, 213–222.

Hudson, J. A., 1981, Wave speeds and attenuation of elastic waves in material containing cracks: *Geophys. J. R. Astron. Soc.* **64**, 133–150.

Hudson, J. A., 1986, A higher order approximation to the wave propagation constants for a cracked solid: *Geophys. J. R. Astron. Soc.* **87**, 265–274.

Hudson, J. A., 1990, Overall elastic properties of isotropic materials with arbitrary distribution of circular cracks: *Geophys. J. Int.* **102**, 465–469.

Kachanov, M., 1992, Effective elastic properties of cracked solids: Critical review of some basic concepts: *Appl. Mech. Rev.* **45**, 304–335.

Kushch, V. I. & Sangani, A. S., 2000, Stress intensity factor and effective stiffness of a solid containing aligned penny-shaped cracks: *Int. J. Solids Struct.* **37**, 6555-6570.

Laws, N. & Dvorak, G. J., 1987, The effect of fiber breaks and aligned penny-shaped cracks on the stiffness and energy release rates in unidirectional composites: *Int. J. Solids Struct.* **23**, 1269–1283.

Mavko, G. & Jizba, D., 1991, Estimating grain-scale fluid effects on velocity dispersion in rocks: *Geophysics* **56**, 1940–1949.

Mavko, G., Mukerji, T. & Dvorkin, J., 1998, *The Rock Physics Handbook: Tools for Seismic Analysis in Porous Media*, Cambridge University Press, Cambridge, pp. 307–309.

Nemat-Nasser, S. & Hori, M., 1993, *Micromechanics: Overall Properties of Heterogeneous Materials*, North-Holland, Amsterdam, pp. 427–431.

Nemat-Nasser, S., Yu, N. & Hori, M., 1993, Solids with periodically distributed cracks: *Int. J. Solids Struct.* **30**, 2071–2095.

Norris, A. N., 1985, A differential scheme for the effective moduli of composites: *Mech. Mater.* **4**, 1–16.

O'Connell, R. J. & Budiansky, B., 1974, Seismic velocities in dry and saturated cracked solids: *J. Geophys. Res.* **79**, 4626–4627.

O'Connell, R. J. & Budiansky, B., 1977, Viscoelastic properties of fluid-saturated cracked solids: *J. Geophys. Res.* **82**, 5719–5735.

Reuss, A., 1929, Berechung der Fliessgrenze von Mischkristallen: *Z. Angew. Math. Mech.* **9**, 55.

Sayers, C. M. & Kachanov, M., 1991, A simple technique for finding effective elastic constants of cracked solids for arbitrary crack orientation statistics: *Int. J. Solids Struct.* **27**, 671–680.

Skempton, A. W., 1954, The pore-pressure coefficients A and B: *Geotechnique* **4**, 143–147.

Smyshlyaev, V. P., Willis, J. R. & Sabina, F. J., 1993, Self-consistent analysis of waves in a matrix-inclusion composite. 3. A matrix containing cracks: *J. Mech. Phys. Solids* **41**, 1809–1824.

Voigt, W., 1928, *Lehrbuch der Kristallphysik*, Teubner, Leipzig, p. 962.

Walsh, J. B., 1969, New analysis of attenuation in partially melted rock: *J. Geophys. Res.* **74**, 4333–4337.

Walsh, J. B., 1980, Static deformation of rock: *ASCE J. Engng. Mech.* **106**, 1005–1019.

Willis, J. R., 1980, A polarization approach to the scattering of elastic waves. Part II: Multiple scattering from inclusions: *J. Mech. Phys. Solids* **28**, 307–327.

Wu, T. T., 1966, The effect of inclusion shape on the elastic moduli of a two-phase material: *Int. J. Solids Struct.* **2**, 1–8 (1966).

Zimmerman, R. D., 1985, The effect of microcracks on the elastic moduli of brittle materials: *J. Mater. Sci. Lett.* **4**, 1457–1460.

Zimmerman, R. D., 1994, Behavior of the Poisson ratio of a two-phase composite material in the high-concentration limit: *Appl. Mech. Rev.* **47**, S38–S44.